Role and location of the unusual redox-active cysteines in the hydrophobic domain of the transmembrane electron transporter DsbD

Federico Katzen* and Jon Beckwith†

Department of Microbiology and Molecular Genetics, Harvard Medical School, Boston, MA 02115

The central hydrophobic domain of the membrane protein DsbD catalyzes the transfer of electrons from the cytoplasm to the periplasm of *Escherichia coli*. Two cysteine residues embedded in transmembrane segments are essential for this process. Our results, based on cysteine alkylation and site-directed proteolysis, provide strong evidence that these residues are capable of forming an intramolecular disulfide bond. Also, by using a combination of two complementary genetic approaches, we show that both cysteines appear to be solvent-exposed to the cytoplasmic side of the inner membrane. These data are inconsistent with earlier topological models that place these residues on opposite sides of the membrane and permit the formulation of alternate hypotheses for the mechanism of this unusual transmembrane electron transfer.

The formation and reduction of protein disulfide bonds plays a role in many important cellular processes, including protein folding, response to oxidative stress, and providing the substrates for DNA synthesis. These processes involve a series of electron-transfer reactions, which have as their ultimate consequence the net transfer of two electrons from two protein cysteines to a variety of acceptors. Such pathways of electron transfer usually require a cascade of disulfide bond oxidation or reduction steps that occur within and between proteins of a pathway (for a recent review see ref. 1).

One pathway that uses a "disulfide cascade" is responsible for the formation of disulfide bonds in many secreted and membrane proteins. The reaction is catalyzed in bacteria by the periplasmic protein DsbA (2). The active site of DsbA contains two essential redox-active cysteines that are joined in a disulfide bond. DsbA promotes disulfide bond formation by removing electrons from substrate proteins and, in the process, reducing its own disulfide bond. For the active form of the enzyme to be regenerated, these electrons are transferred to the protein DsbB, which contains two pairs of redox-active cysteines. The two DsbB pairs of cysteines act in a coordinate fashion to transfer electrons to quinones in the cytoplasmic membrane (3, 4). The disulfide cascade portion of this pathway thus involves transfer of electrons between four pairs of cysteines: one pair in the substrate, one in DsbA, and two in DsbB. All of these steps take place in a single cellular compartment, the bacterial periplasm.

Processes responsible for the reduction of disulfide bonds also use disulfide cascades (5). Whereas disulfide bond formation is largely limited to extracytoplasmic compartments, disulfide bond reduction pathways have been described in both cytoplasmic and extracytoplasmic compartments. For example, in the cytoplasm, the reduction of ribonucleotide reductase can be achieved by the transfer of electrons from the cysteines of thioredoxin reductase to the cysteines of thioredoxin and thence to the cysteines of ribonucleotide reductase.

In the bacterial periplasm, an important disulfide reduction process is that required for disulfide bond isomerization, the correction of inappropriately formed protein disulfide bonds. Disulfide bond isomerization involves a more complicated disulfide cascade, which, in contrast to other known cascades, requires an exceptional transfer of electrons from the cytoplasm to the

periplasm via the intermediary of the membrane protein, DsbD (formerly called DipZ) (6, 7). DsbD is the only protein capable of performing a thiol–disulfide bond exchange reaction with substrates on opposite sides of a membrane. It transfers reducing potential from cytoplasmic thioredoxin to a variety of periplasmic acceptors, such as the disulfide bond isomerase DsbC, responsible for shuffling wrongly formed disulfide bonds in proteins, and to a member of the cytochrome *c* maturation pathway, CcmG (8–10). In *dsbD* null mutants, wrongly formed disulfide bonds accumulate in periplasmic proteins with more than two cysteines, because of the absence of reduced (active) DsbC (9, 11). In addition, these cells are depleted of *c*-type cytochromes because of disruption of the cytochrome *c* maturation pathway (6).

DsbD is composed of three domains: an N-terminal immunoglobulin-like domain (α), a central hydrophobic core (β) with eight transmembrane segments (TM segments), and a C-terminal periplasmic domain (γ), which appears to be a member of the thioredoxin superfamily (12–17) (Fig. 1*A*). Each of these domains contains a pair of essential cysteines. Based on algorithms that predict TM segments and on gene fusion analyses, we and others have suggested that the essential cysteines 163 and 285 located in the β domain lie on opposite sides of the membrane within TM segments (12–14) (Fig. 1 *A* and *B*).

Electron transfer by DsbD involves sequential reduction and oxidation of its three structural domains, in which reducing potential is transferred from cytoplasmic thioredoxin to β, then successively to γ and α, and thence to periplasmic substrates (10, 18). The ability to trap and identify several of the expected reaction intermediates validates the model (10, 19). In particular, the identification of the mixed disulfide intermediate between cysteine 32 of cytoplasmic thioredoxin and cysteine 163 of β supports the hypothesis that this residue faces the cytoplasmic side of the membrane.

The predicted location of the essential cysteines of β poses several unsolved questions about the mechanism of transmembrane electron transfer. For example, can these two seemingly membrane-embedded cysteines form a disulfide bond? How can the electrons be transferred between these cysteine residues if they face opposite sides of the membrane? In this work we revisit these issues. Our results answer some of these questions but, unexpectedly, are inconsistent with the proposed topological structure of DsbD. These results lead us to propose alternate models for the mechanism of transmembrane electron transfer.

Methods

Strains, Plasmids, Media, and Other Reagents. Strains and plasmids used in this work are listed in Table 1. *Escherichia coli* cells were grown in NZ medium (8) at 37°C, with the appropriate antibi-
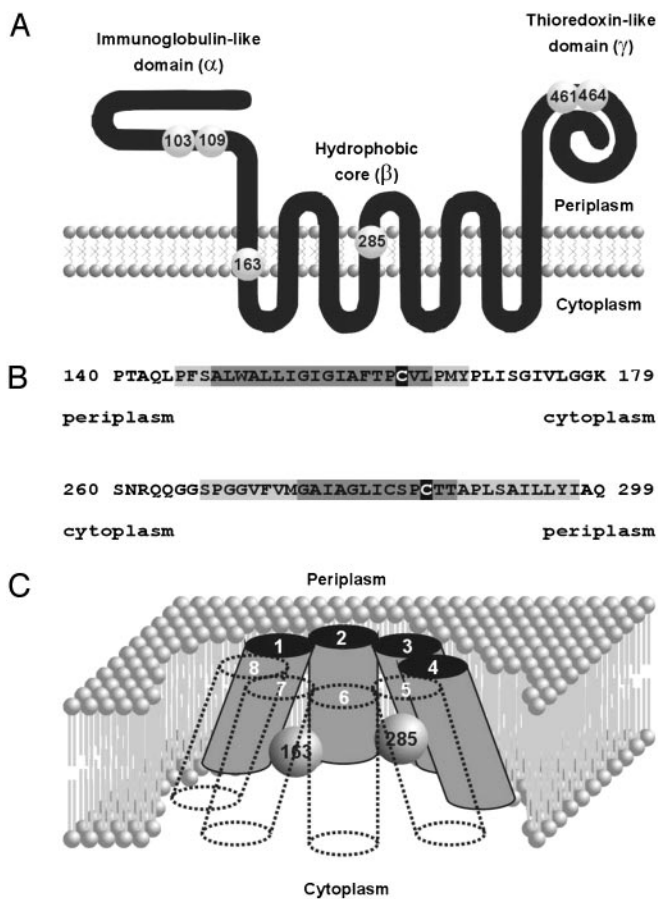

MICROBIOLOGY

Fig. 1. Proposed DsbD topology. (*A*) Diagram showing the proposed three-domain structure of DsbD and the formerly proposed location of the essential cysteines (numbered spheres). (*B*) Blowout of the first and fourth predicted TM segments. Numbers represent the position of the sequence in the mature form of DsbD. Sequences with a darker gray shadow are predicted to be part of TM segments by all the algorithms used (see *Methods*). Light gray-shadowed sequences are predicted to be part of TM segments by a subset of them. Cysteines 163 and 285 are indicated on black. (*C*) Newly proposed topology for the β domain of DsbD. White numbers correspond to each of the eight TM segments. Numbered spheres represent the redox-active cysteines. Other models are also consistent with our results (see text).

otics. Plasmid-encoded variants of DsbD were induced with 0.2% arabinose.

To generate a plasmid encoding a DsbD variant with a thrombin site at the second cytoplasmic loop, a fragment from pFK093 was amplified by using the diverging phosphorylated primers 1throm2cyto (5′-ACCACGGGGAAGTCGCCAA-CAGGGCGGCTCACCTGGCGGTGTGTTTGTTA-3′) and 1throm2cytoRC (5′-ACCAGGCTGCCATTGCTCATCA-ACGTGAGACGTGTTTGCAGCGAAGAGGG-3′). The product was self-ligated, and codons for cysteines 103, 109, 461, and 464 were replaced by those for alanines generating plasmid pFK277.

To construct a plasmid encoding a C-terminal c-Myc-tagged variant of a DsbD devoid of the γ domain harboring two TEV recognition sites in tandem between the α and β domains, a fragment from pFK093 was amplified by using the diverging phosphorylated primers TEV1Tandem_F (5′-ACTTCCAGTC-AGGTAGTGAGAATCTCTACTTCCAGTCAGGCTCC-GGTAGCGGTAGTCAATTGCCCTTTTTCCGCGCTCT-GGGCGTTGTTGATCGG-3′) and TEV1Gly_Ser_B (5′-ACAGGTTTTCACTACCGCTACCGGAGCCCGCGGTG-

Table 1. Strains and plasmids used in this work

Strain/plasmid*	Relevant genotype or features
Strains	
FED126 (10)	*araD*139 (*araABC-leu*)7679 *galU galK* Δ(*lac*)X74 *rpsL thi* Δ*dsbD*
FED513 (10)	FED126 *trxB*∷Kan[r]
Plasmids	
pFK060 (10)	pBAD18 with MalF′-β-c-Myc
pFK072	pBAD18 with MalF′-β$_{C163A}$-c-Myc
pFK073	pBAD18 with MalF′-β$_{C285A}$-c-Myc
pFK091 (10)	pBAD33 with α$_{C109A}$-His$_6$
pFK093 (10)	pBAD18 with DsbD
pFK253	pBAD18 with MalF′-β$_{C163/285A}$-c-Myc
pFK269	pBAD18 with αβ-c-Myc$_{C103/109A}$
pFK270	pBAD18 with αβ-c-Myc$_{C103/109/163A}$
pFK271	pBAD18 with αβ-c-Myc$_{C103/109/285A}$
pFK272	pBAD18 with αβ-c-Myc$_{C103/109/163/285A}$
pFK277	pBAD18 with DsbD$_{C103/109/461/464A}$ with thrombin site

*Except where indicated (10), the source of the strain or plasmid is the present work.

GGCTGCTCTTGCTGCGGAACAGACACAGGCTGTGG-CGC-3′). The product was self-ligated. A *Blp*I–*Sph*I DNA fragment from the resulting plasmid was replaced by that fragment from pFK060, generating plasmid pFK269.

When indicated, the cysteines of the described constructs were mutated to alanines by using the QuikChange Site-Directed Mutagenesis Kit (Stratagene) as directed by the manufacturer. All the constructions were verified by DNA sequencing. Non-essential DsbD cysteines located in the leader peptide and at position 282 were replaced by alanines in all DsbD derivatives.

Antibodies have been described (10).

Thiol-Redox State Analyses. To determine the *in vivo* redox state of the proteins, free thiols were alkylated with the high-molecular-weight reagent malPEG (mPEG-MAL, M_r 5,000; Nektar Therapeutics, San Carlos, CA). Basically, we used the same alkylation protocol used previously (12) by using 0.5-ml culture samples, replacing 4-acetamido-4′-maleimidylstilbene-2,2′-disulfonic acid by malPEG at a final concentration of 3 mM, and diluting the sample with SDS/sample buffer (1:1) before gel loading. The stock solution of malPEG (50 mM in DMSO) was stored at −80°C for up to 6 months. Alkylation of exposed cysteines on vesicles was performed with 6 mM malPEG.

Digestion with Thrombin. Cells (1 ml) were precipitated with tri-chloroacetic acid (TCA), resuspended in 0.5 ml of 1 M Tris·HCl, pH 8/20 mM *N*-ethylmaleimide (Sigma-Aldrich), and incubated for 1 h at room temperature. *N*-ethylmaleimide-alkylated samples were centrifuged, washed with 1 ml of PBS, and resuspended in 0.5 ml of PBS with or without 10 units of thrombin (Amersham Bio-sciences). Samples were incubated overnight at 30°C, centrifuged, and resuspended in SDS/sample buffer.

Preparation of Spheroplasts. Five milliliters of cells was harvested at midlogarithmic phase, washed with ice-cold buffer (50 mM Tris·HCl, pH 8/1 mM CaCl$_2$/18% sucrose), and resuspended in 1 ml of the same buffer. Two 0.5-ml aliquots were carefully added into tubes already containing ice-cold 1 μl of 0.5 M EDTA, 5 μl of 100 μg/ml lysozyme, and 50 μl of 50 mM malPEG. Samples were incubated on ice for 1 h, TCA-precipitated, washed with acetone, and resuspended in SDS/sample buffer containing 50 mM DTT, which quenches the residual activity of malPEG. One

of the samples was subjected to two 5-sec sonication pulses on ice during the alkylation time.

Preparation of Vesicles. One hundred milliliters of midlogarithmic-phase cells was centrifuged and resuspended in 20 ml of 50 mM potassium phosphate buffer, pH 8. Vesicles were obtained by passing the cells through a French pressure cell [1,200 psi (1 psi = 6.89 kPa)]. Cell debris was removed by centrifugation (12,000 × g for 10 min at 4°C). Vesicles (300 μl) were incubated overnight at 30°C with or without 50 units of tobacco etch virus (TEV) protease (Invitrogen) in the presence of 1 mM DTT and 50 μl of 20× TEV buffer in a final volume of 1 ml. After proteolysis, malPEG was added, or not, to the samples at a concentration of 6 mM. Samples were incubated at room temperature for 1 h, TCA-precipitated, acetone-washed, and resuspended in SDS/sample buffer containing 50 mM DTT.

Sequence Analyses. TM segment prediction analyses were performed by using TMPRED (www.ch.embnet.org/software/TMPRED_form.html), TMHMM (www.cbs.dtu.dk/services/TMHMM-2.0) (20), TOPPRED (http://bioweb.pasteur.fr/seqanal/interfaces/toppred.html), SOSUI (http://sosui.proteome.bio.tuat.ac.jp/cgi-bin/sosui.cgi?/sosui_submit.html), and DAS (www.sbc.su.se/≈miklos/DAS) (21). Helix amphipathicity was estimated by using HELIXDRAW V1.0 (http://bioinf.man.ac.uk/≈gibson/HelixDraw/helixdraw.html).

Results

The Catalytic Cysteines of DsbDβ Can Form an Intramolecular Disulfide Bond.

The thiol–disulfide redox state of a protein can be determined by denaturing the molecule under nonreducing conditions and assessing the accessibility of its free thiol groups to an alkylating reagent. Two cysteines that are engaged in a disulfide bond are usually refractory to alkylation.

Previously, we attempted to determine the redox state of the β domain of *E. coli* DsbD by alkylating its free cysteines with 4-acetamido-4′-maleimidylstilbene-2,2′-disulfonic acid (10). However, the gel-mobility shifts on alkylation were not clear-cut enough to draw conclusions. Here we use a higher-molecular-weight (5,000) alkylating reagent, malPEG (see *Methods*), to assess the redox state of β.

We expressed four plasmid-encoded variants of the β peptide harboring two, one, or none of the essential cysteines, either in a *dsbD* null strain or in a double-knockout strain, *dsbD*, *trxB*. In this latter strain, the absence of thioredoxin reductase (*trxB*) results in the accumulation of oxidized thioredoxins in the cytoplasm. The oxidized thioredoxins now promote the formation of disulfide bonds, a reversal of their normal role (22), a process that also appears to occur with their substrate, DsbD (10).

When malPEG is used, the alkylated and nonalkylated isoforms of β are clearly distinguishable (Fig. 2). In the *dsbD* background, the mobility shift of the four different variants correlates well with the number of cysteines that they harbor, indicating that both residues, Cys-163 and Cys-285, are accessible to alkylation (Fig. 2, lanes 1–5). However, in a double mutant, *dsbD*, *trxB*, the construct containing both cysteines is not alkylated (Fig. 2, lanes 6–9). This lack of reactivity of the cysteines can be reversed by preincubating the cells with the thiol-reductant DTT (not shown). These results suggest that either (*i*) both cysteines can form an intramolecular disulfide bond or that (*ii*) these residues can be reversibly and simultaneously blocked *in vivo* by a small thiol-reactive molecule. We note that alkylation with one or two bulky molecules of malPEG strongly lowers the total amount of detectable protein (Fig. 2, compare lanes 2 with lanes 3–5, and lanes 6 and 9 with lanes 7 and 8) perhaps because of constraints on transfer of proteins to the nitrocellulose membrane imposed by the reagent.

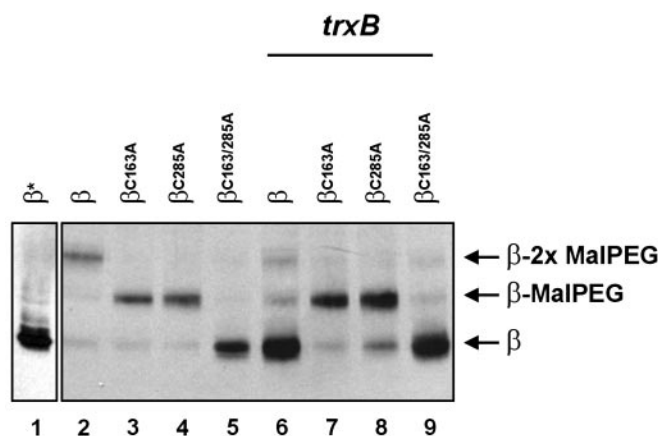One way to unequivocally distinguish between the two interpretations of our results is to cleave the presumed "oxidized"

Fig. 2. *In vivo* redox state of the β domain of DsbD. Cells expressing the designated derivatives were grown in the presence of 0.2% arabinose and subjected to TCA precipitation and malPEG alkylation (with the exception of lane 1, marked with an asterisk). Samples were reduced with 25 mM DTT before loading. Proteins were separated by SDS/PAGE and visualized by Western blotting using anti-c-Myc antibodies. The strain background used in lanes 1–5 was FED126. All other lanes used FED513. The following plasmids were used: pFK060 (lanes 1, 2, and 6), pFK072 (lanes 3 and 7), pFK073 (lanes 4 and 8), and pFK253 (lanes 5 and 9). Binding of malPEG to proteins appears to hinder their transfer to the nitrocellulose membrane (see text).

protein somewhere between the two cysteine residues. If these two cysteines were joined by a disulfide bond, both halves of the protein would remain covalently bound after cleavage.

We constructed a DsbD derivative harboring a thrombin cleavage site inserted in the second cytoplasmic loop. This protein retained full activity and was readily cleavable by thrombin (not shown). To ensure that the only possible intramolecular disulfide bond is that between Cys-163 and Cys-285, we replaced the essential cysteines in the α and γ domains with alanines. This variant, although lacking DsbD activity because of the absence of functional α and γ domains, maintains its β domain intact.

This construct was expressed in the double mutant, *dsbD*, *trxB*. To avoid artifactual thiol–disulfide exchange reactions during extract preparation, cells were TCA-precipitated and free thiols were alkylated with *N*-ethylmaleimide as indicated in *Methods*. For technical reasons, SDS is omitted at this stage. As a result, proteins may not be completely unfolded and not all free thiol groups may be inactivated by alkylation. We have observed that full-length DsbD, expressed from pBAD plasmids, frequently migrates as two bands (Fig. 3, lanes 1–3), which are differentially detected by anti-α (Fig. 3A) and anti-γ antisera (Fig. 3B). They probably represent different denatured conformations of the protein, and their ratios depend on the time of incubation with SDS/sample buffer (data not shown).

We find that a significant fraction of the DsbD variant with the thrombin site remains intact after digestion with thrombin (Fig. 3, lane 3). However, DTT treatment results in the complete disappearance of this molecule and is accompanied by an increase in the amount of two smaller polypeptides, each of which is detected by only one of the antisera (Fig. 3, lane 4). Note that the anti-α antiserum does not seem to recognize the full-length, nonreduced form of DsbD as well as it recognizes the reduced αβ′ protein (compare the intensity of the bands in Fig. 4A, lanes 2 and 4). These results provide strong evidence that the two halves of the protein are held together by a disulfide bond. Because the presence or absence of the disulfide bond depends on the state of cytoplasmic thioredoxins, which are responsible for transfer of electrons to DsbD, we suggest that formation of a disulfide bond between cysteines 163 and 285 of the β domain is part of the mechanism of the transmembrane electron transfer by DsbD.
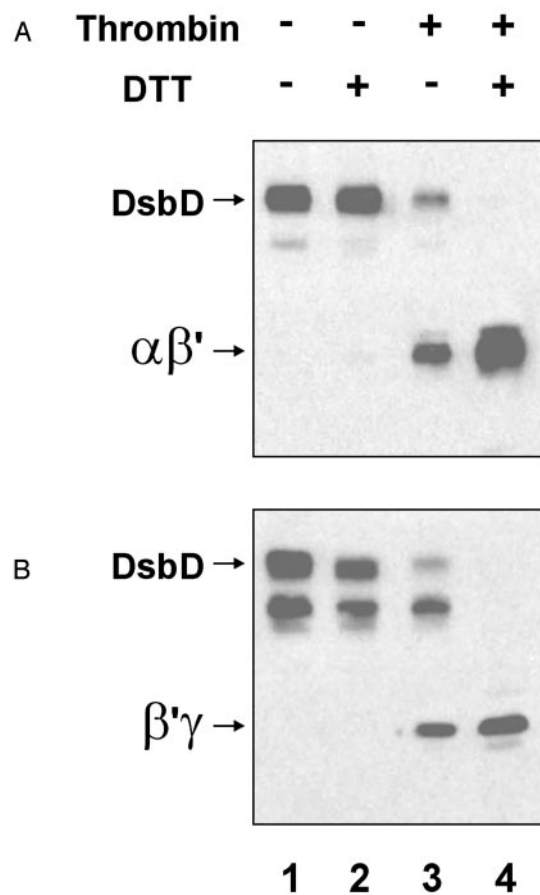
MICROBIOLOGY

Fig. 3. Thrombin digestion of a modified variant of DsbD. FED513 cells containing the plasmid pFK277 were grown as indicated before and alkylated with *N*-ethylmaleimide as specified in *Methods*. Samples were digested or not by thrombin protease and resuspended in SDS/sample buffer. When indicated, aliquots were reduced with 50 mM DTT. Proteins were visualized by Western blotting using antibodies against the α (*A*) and γ (*B*) peptides.

The Catalytic Cysteines of DsbDβ Are Protected from Alkylation in Intact Spheroplasts.

The formation of the disulfide bond in the β domain of DsbD raises questions about the actual location of the two cysteines in the topological structure of the protein. One simple way to tackle this problem is to prepare spheroplasts and examine which cysteines can be modified by a membrane-impermeant alkylating reagent that should only react with surface-exposed cysteine residues. Cytoplasmic cysteine residues should become accessible to alkylation only when lysis of spheroplasts is induced, and membrane-embedded cysteines should never be modified by the reagent.

We prepared spheroplasts from a *dsbD*-null strain expressing the same β variants used in the previous section by using the EDTA/lysozyme treatment described in *Methods*. As a control for the integrity of spheroplasts we used cytoplasmic thioredoxin 1, which should remain protected from alkylation. As a positive control, we used a single-cysteine-containing variant of the α domain of DsbD that is exported to the periplasmic space.

Our results show that essentially no cysteine residue of β is accessible to alkylation on the surface of spheroplasts irrespective of the β variant used (Fig. 4 *B* and *D*, lanes 1–4). However, when the spheroplasts were lysed, either cysteine of β could be alkylated, although this alkylation was seen only when the two single cysteine variants were used (Fig. 4*B*, lanes 5 and 6). This failure to alkylate the two cysteines in the WT isoform of β (Fig. 4*B*, lane 5) is likely caused by oxidation of these residues, which occurs during sphero-
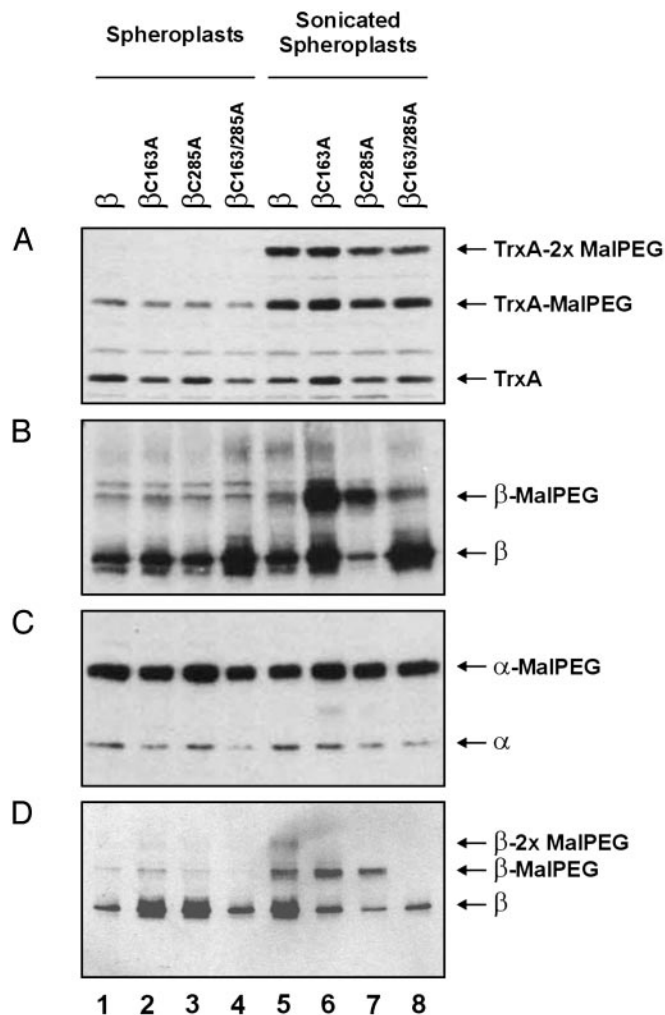

Fig. 4. Alkylation of exposed cysteines on spheroplasts. Spheroplasts from FED126 cells, expressing the designated constructs, were prepared and alkylated as indicated in *Methods*. Proteins were separated by SDS/PAGE and visualized by Western blotting using the following antibodies: anti-thioredoxin 1 (TrxA) (*A*), anti-c-Myc epitope (*B* and *D*), or against the α peptide (*C*). The following plasmids were used: pFK060 (lanes 1 and 5), pFK072 (lanes 2 and 6), pFK073 (lanes 3 and 7), pFK253 (lanes 4 and 8), and pFK091 (all lanes). Cells used in *D* were incubated with 50 mM DTT before processing. Samples for lanes 5–8 were sonicated as indicated in *Methods*.

plast preparation. Such artifactual oxidation is common and occurs, for example, in the purification of DsbD, which is ultimately obtained as a completely oxidized protein (unpublished data). Therefore, it is reasonable to expect that exposure of cells to a thiol reductant during the first stages of spheroplast preparation should at least partially counteract the oxidative effect. Accordingly, preincubation of cells with DTT made the WT variant readily accessible to the reagent when the spheroplasts were subjected to sonication (Fig. 4*D*, lanes 5–8), but did not alter the cysteine accessibility to malPEG of the constructs in intact spheroplasts (Fig. 4*D*, lanes 1–4). The spheroplasts appear to remain relatively intact during the course of the experiment as judged by the alkylation state of cytoplasmic thioredoxin 1 (Fig. 4*A*, lanes 1–4). Alkylation of thioredoxin on sonication indicates that the procedure effectively disrupts the membrane and releases the cytoplasmic content. Reaction of one malPEG molecule with thioredoxin appears to partially hinder the binding of a second one as indicated by the prominent band of hemi-alkylated thioredoxin. This effect may be due to the close spacing of the cysteines (CGPC) and the bulkiness
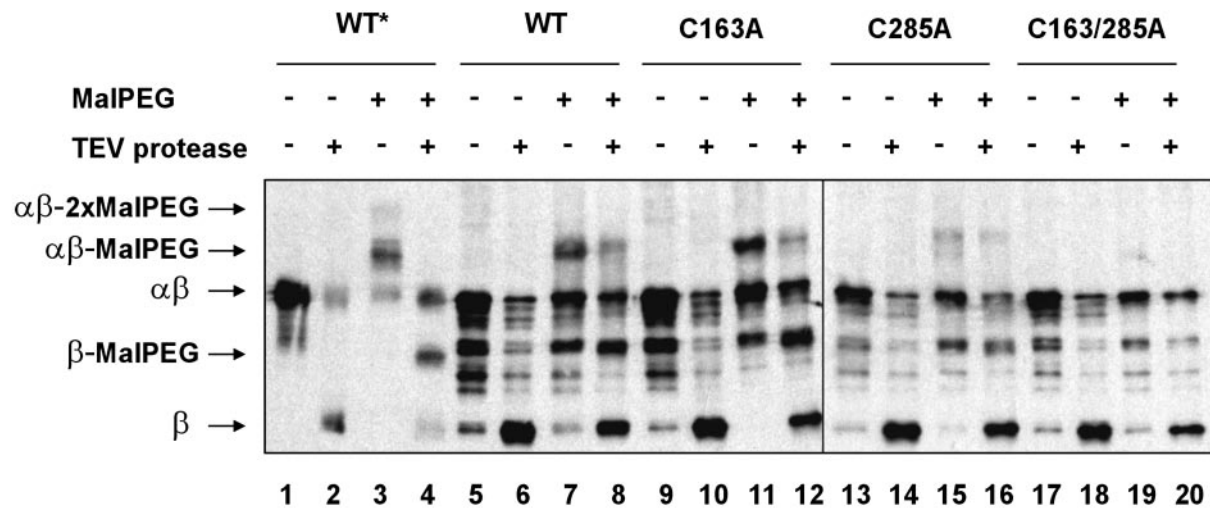
Fig. 5. Alkylation of exposed cysteines on vesicles. Vesicles from FED126 cells expressing the designated constructs were prepared as indicated in *Methods*. Vesicles were incubated with TEV protease and malPEG as depicted by symbols + and −. Proteins were visualized by Western blotting using antibodies that react against the c-Myc epitope. The following plasmids were used: pFK269 (lanes 1–8), pFK270 (lanes 9–12), pFK271 (lanes 13–16), and pFK272 (lanes 17–20). The asterisk indicates that whole TCA-precipitated cells were used, instead of vesicles. Thus, bands on lanes 1–4 show the electrophoretic mobility for each of the possible species.

of the alkylating agent, malPEG. The results with the positive control for this experiment (DsbDα) indicate that protein alkylation occurs efficiently whether or not the spheroplasts are sonicated (Fig. 4C). The simplest explanation for these results is that, contrary to the topological prediction models, both cysteine residues face the cytoplasm.

Both Catalytic Cysteines of DsbDβ Embedded in the Membrane of Inside-Out Vesicles Can Be Modified by the Addition of a Membrane-Impermeant Alkylating Reagent. To obtain additional evidence for the surprising findings on the location of the two cysteines, we have used an approach complementary to the spheroplast studies. Because the two cysteines of β are not accessible to alkylation on the periplasmic face of the cytoplasmic membrane, we can ask whether they are accessible on the cytoplasmic face of the membrane by doing analogous experiments with inside-out (cytoplasmic face of the membrane out) vesicles. The techniques used for preparing inside-out vesicles usually also yield right-side-out vesicles. We developed a strategy that allowed us to distinguish effects of alkylation on the two classes of vesicle in a single preparation. First, to prevent folding problems, we studied the αβ peptide, rather than the β domain alone. The former peptide contains the native DsbD signals that ensure correct membrane insertion. To avoid confusion between the cysteines of the α and β domains, cysteines 103 and 109 of the α domain were replaced by alanines. Finally, two TEV protease recognition sites were inserted in tandem between the α and β domains. These cleavage sites are located on the periplasmic face of the membrane in whole cells and, therefore, are accessible to TEV protease with the right-side-out vesicles but not with the inside-out vesicles. Cleavage of these sites should permit a clear distinction between the αβ peptide correctly inserted in inside-out vesicles and other unwanted isoforms. Incorporation of these cleavage sites does not affect the protein's activity (not shown). Only those isoforms that are resistant to the TEV treatment will be relevant for the analysis.

To interpret the results correctly, we first needed to determine the electrophoretic mobility of each of the possible species that result from TEV digestion. We did this by first using samples of whole cells that had been previously lysed and denatured on TCA precipitation. We could distinguish five of six possible species on a Western blot (Fig. 5, lanes 1–4). The remaining one,

the β peptide bound to two molecules of malPEG, probably comigrates with noncleaved, nonalkylated αβ. Again, we observed that binding of malPEG strongly lowers the amount of detectable protein. The larger the protein is, the more evident this effect becomes (data not shown). For example, only tiny amounts of doubly alkylated αβ could be observed (Fig. 5, lane 3). Therefore, it would not be adequate to compare relative amounts of different species among the lanes.

Based on these findings, vesicles from strains containing four variants of the αβ peptide harboring two, one, or none of the central cysteines were first incubated with or without TEV protease, and then they were incubated with or without malPEG. If the central cysteines of the β peptide faced the cytoplasmic side of the membrane, cysteines from intact, but not from cleaved, αβ should be alkylated. Conversely, if at least one of the cysteines faced the periplasmic side of the membrane, alkylated isoforms of the cleaved β peptide should be readily detected.

Western blots prepared from vesicles treated by this procedure accumulate a number of bands. Although cleavage of β takes place efficiently, no band corresponding to that of alkylated cleaved β was observed (Fig. 5, compare lane 4 with lanes 6–20). This result indicates that αβ, exhibiting its periplasmic face outside on in right-side-out vesicles, is subject to cleavage by TEV protease but does not have either cysteine exposed on this face of the membrane. Conversely, alkylation of both central cysteines of intact αβ was observed on TEV protease incubation (Fig. 5, lanes 8, 12, and 16). Thus, inside-out vesicles, in which the TEV protease site is not exposed, do expose the cysteines of β to alkylation. Because both cysteine residues can be readily alkylated in mutants C163A and C285A (Fig. 5, lanes 11, 12, 15, and 16), our inability to detect doubly alkylated αβ may be the result of inefficient transfer to the nitrocellulose membrane as explained above (Fig. 5, lanes 7 and 8).

We observed a slight decrease in the amount of alkylated αβ peptide on TEV protease digestion (Fig. 5, lanes 8, 12, and 16). This effect is not accompanied by the generation of a band corresponding to an alkylated β band, and it is observed also with the mutant C285A, which conserves the Cys-163 that interacts with cytoplasmic thioredoxin (Fig. 5, compare lanes 15 and 16). This effect may be due to a minor nonspecific proteolytic activity that accompanies the enzyme preparation.

Although we cannot explain the origin of certain of the bands

seen on these gels, the key results on the protease accessibility of the alkylated and nonalkylated forms of the $\alpha\beta$ polypeptide provide support for our interpretation of the findings with spheroplast preparations. In summary, our results suggest that the catalytic cysteines of the β domain are exposed to the external milieu on inside-out vesicles, indicating that these residues are likely to be facing the cytoplasmic side of the membrane in living cells.

Discussion

In this article, we describe features of a process of electron transfer from cytoplasm to periplasm carried out by the cytoplasmic membrane protein DsbD. This protein promotes transmembrane electron transfer by using two redox-active cysteines located in the protein's hydrophobic core.

First, our data provide strong evidence that these two cysteines are capable of forming an intramolecular disulfide bond. These findings strengthen the previous suggestions that the mechanism of electron transfer is based on a series of thiol–disulfide bond exchange reactions (10). Second, our results, based on complementary approaches, are consistent with a model in which these cysteines face the cytoplasmic face of the membrane.

Although our results do not rule out the possibility that these two cysteines are embedded in the membrane in such a way that they are still accessible to the alkylating agent (see below), they are inconsistent with the previously proposed topological model for DsbD, which places these residues on opposite faces of the lipid bilayer (12–14). That model would have required a major conformational change of the protein to explain how these distant cysteines form a disulfide bond. Our findings simplify the model in the sense that, because both cysteine residues appear to be exposed to the same cell compartment, no need exists to postulate a major rearrangement for the formation of this bond.

A closer examination of the topological prediction for DsbD from hydropathy profiles, reveals that, whereas Cys-163 is predicted to be located relatively close to the C-terminal end of the first TM segment, the positions of the borders of the fourth TM segment, where Cys-285 is found, are not so obvious (Fig. 1B). In addition, hydropathy profiles, obtained by using the DAS and SOSUI TM prediction algorithms, reveal a relatively deep hydrophilic valley around position 285 in TM4 (data not shown). This region exhibits local amphipathicity when the segment is modeled as an α-helix (data not shown). Therefore, it is tempting to propose that these residues are solvent-accessible either by facing the cytoplasmic side of the membrane or by extending into a hydrophilic membrane-embedded cavity (Fig. 1C).

Our findings are consistent with a reaction between thioredoxin and the β domain of DsbD that is no different from other thiol–disulfide bond exchanges, in which electrons are transferred from a pair of thiol groups in one protein to a pair of oxidized cysteines in a second protein, all taking place in a hydrophilic environment. However, the tantalizing question concerning the transfer of reducing potential from β to γ remains unsolved. How does γ, located in the periplasm, access the two cysteines facing the cytoplasm? We can imagine at least two ways in which this can be accomplished. First, the γ domain or only its helix II and its immediate loop where the two cysteines are presumably located (17) might be imported across or inserted into the membrane, thereby allowing thiol–disulfide bond exchange between the two cysteine pairs. Such a process would face a large energy barrier associated with translocation of charged residues across the membrane. However, this type of translocation is certainly conceivable because insertion of charged helices into a membrane and translocation of a water-soluble domain across planar phospholipid bilayers have already been reported for colicins and the diphtheria toxin, respectively (23, 24). Our previous failure to find a mixed disulfide intermediate between β and γ (10) may be due to its short-lived nature, a consequence of the unfavorable energy threshold required for this proposed interaction.

We cannot rule out the possibility that, analogous to the interaction of quinones with DsbB (3), a small molecule is involved in the transfer of electrons between β and γ. Although an in vitro system using purified DsbD components has been developed recently, the hypothesis of the existence of additional electron-transporting cofactors could neither be proved nor ruled out (18).

Finally, it is still possible that a major rearrangement of the hydrophobic core occurs, thereby allowing thiol–disulfide bond exchange in the periplasmic space. Although our results do not favor this hypothesis, it is conceivable that such a conformational change does not persist long enough to allow cysteine alkylation. Structural studies, notoriously difficult with membrane proteins, may be required to resolve some of these questions.

1. Kadokura, H., Katzen, F. & Beckwith, J. (2003) *Annu. Rev. Biochem.* **72**, 111–135.
2. Bardwell, J. C., McGovern, K. & Beckwith, J. (1991) *Cell* **67**, 581–589.
3. Bader, M., Muse, W., Ballou, D. P., Gassner, C. & Bardwell, J. C. (1999) *Cell* **98**, 217–227.
4. Kadokura, H. & Beckwith, J. (2002) *EMBO J.* **21**, 2354–2363.
5. Aslund, F. & Beckwith, J. (1999) *J. Bacteriol.* **181**, 1375–1379.
6. Crooke, H. & Cole, J. (1995) *Mol. Microbiol.* **15**, 1139–1150.
7. Missiakas, D., Schwager, F. & Raina, S. (1995) *EMBO J.* **14**, 3415–3424.
8. Rietsch, A., Belin, D., Martin, N. & Beckwith, J. (1996) *Proc. Natl. Acad. Sci. USA* **93**, 13048–13053.
9. Rietsch, A., Bessette, P., Georgiou, G. & Beckwith, J. (1997) *J. Bacteriol.* **179**, 6602–6608.
10. Katzen, F. & Beckwith, J. (2000) *Cell* **103**, 769–779.
11. Joly, J. C. & Swartz, J. R. (1997) *Biochemistry* **36**, 10067–10072.
12. Stewart, E. J., Katzen, F. & Beckwith, J. (1999) *EMBO J.* **18**, 5963–5971.
13. Chung, J., Chen, T. & Missiakas, D. (2000) *Mol. Microbiol.* **35**, 1099–1109.
14. Gordon, E. H., Page, M. D., Willis, A. C. & Ferguson, S. J. (2000) *Mol. Microbiol.* **35**, 1360–1374.
15. Haebel, P. W., Goldstone, D., Katzen, F., Beckwith, J. & Metcalf, P. (2002) *EMBO J.* **21**, 4774–4784.
16. Goulding, C. W., Sawaya, M. R., Parseghian, A., Lim, V., Eisenberg, D. & Missiakas, D. (2002) *Biochemistry* **41**, 6920–6927.
17. Kim, J. H., Kim, S. J., Jeong, D. G., Son, J. H. & Ryu, S. E. (2003) *FEBS Lett.* **543**, 164–169.
18. Collet, J. F., Riemer, J., Bader, M. W. & Bardwell, J. C. (2002) *J. Biol. Chem.* **277**, 26886–26892.
19. Krupp, R., Chan, C. & Missiakas, D. (2001) *J. Biol. Chem.* **276**, 3696–3701.
20. Krogh, A., Larsson, B., von Heijne, G. & Sonnhammer, E. L. (2001) *J. Mol. Biol.* **305**, 567–580.
21. Cserzo, M., Wallin, E., Simon, I., von Heijne, G. & Elofsson, A. (1997) *Protein Eng.* **10**, 673–676.
22. Stewart, E. J., Aslund, F. & Beckwith, J. (1998) *EMBO J.* **17**, 5543–5550.
23. Zakharov, S. D. & Cramer, W. A. (2002) *Biochim. Biophys. Acta* **1565**, 333–346.
24. Oh, K. J., Senzel, L., Collier, R. J. & Finkelstein, A. (1999) *Proc. Natl. Acad. Sci. USA* **96**, 8467–84670.